

DESY SR-81/12
October 1981

Eigentum der Property of	DESY	Bibliothek library
Zugang: Accessions:	17. Jan. 2002	
Keine Ausleihe Not for loan		

THE NEW MULTI-PURPOSE TWO-AXIS DIFFRACTOMETER
FOR SYNCHROTRON X-RAYS AT DORIS

by

U. Bonse

Institut für Physik, Universität Dortmund

K. Fischer

Fachrichtung Kristallographie, Universität des Saarlandes

DESY behält sich alle Rechte für den Fall der Schutzrechtserteilung und für die wirtschaftliche Verwertung der in diesem Bericht enthaltenen Informationen vor.

DESY reserves all rights for commercial use of information included in this report, especially in case of apply for or grant of patents.

To be sure that your preprints are promptly included in the
HIGH ENERGY PHYSICS INDEX ,
send them to the following address (if possible by air mail) :

DESY
Bibliothek
Notkestrasse 85
2 Hamburg 52
Germany

The new multi-purpose two-axis diffractometer
for Synchrotron X-rays at DORIS

U. Bonse⁺⁾ and K. Fischer⁺⁺⁾

⁺⁾ Institut für Physik, Universität Dortmund,
Postfach 50 05 00, D-4600 Dortmund 50
Fed. Rep. of Germany

⁺⁺⁾ Fachrichtung Kristallographie, Universität des Saarlandes
Im Stadtwald, D-6600 Saarbrücken 11
Fed. Rep. of Germany

The new two-axis diffractometer recently installed at the storage ring DORIS at DESY/HASYLAB, Hamburg, is described.

The instrument has especially been designed to make best use of the outstanding properties of synchrotron X-rays, i.e. high collimation, polarization, wavelength (energy) tunability, and overall high intensity.

Its central feature is a rigid two-crystal diffractometer bench which is mounted on a swing so that it can be rotated about the axis of the incident beam. Thus the diffraction plane of the bench can assume any orientation between horizontal and vertical which permits to exploit conveniently the polarization of the source. The orientational flexibility of the two-crystal bench is complemented by a preceding monochromator the diffraction plane of which can independently be chosen between horizontal and vertical.

A solid state detector separately mounted on another swing of corresponding design can freely follow the movement of the two-crystal bench without direct mechanical coupling to it. Thus the vibrational noise at the bench is kept low.

The double-crystal bench is capable of carrying a pair of medium size temperature stages enclosing the crystals.

All essential movements including vertical adjustment of the whole instrument with respect to the synchrotron beam feature fully automatized operation through an on-line computer.

Due to its versatile and flexible design the diffractometer can be employed for a great variety of different experiments such as high resolution two-crystal topography and diffraction line analysis, high resolution small angle scattering, Compton scattering, energy and momentum resolved X-ray scattering, anomalous dispersion measurements, fluorescence and ordinary X-ray spectroscopy etc.

1. Introduction

With the decision to build five more primary beam ports at HASYLAB also the development and construction of additional X-ray instrumentation was initiated. Since the characteristics of a synchrotron source differ in many respects from those of an ordinary X-ray tube it was judged better from the very beginning not only to transfer conventional X-ray equipment to the storage ring but also to try to build new instruments more capable to make proper use of the unique properties of synchrotron radiation like extreme beam collimation, polarization and wavelength tunability.

Furthermore, some larger instruments had to be designed as "users instruments", i.e. allowing for the circumstance that they will be used by several research groups performing quite different experiments, implying further that the operation of such an instrument should be easy and safe even by - as a whole - unexperienced users.

One of these new user instruments is the two-axis diffractometer [1] to be described below. It is essentially a versatile two-crystal diffractometer equipped with an additional fore-crystal as monochromator. The instrument is capable of operation in any plane between horizontal and vertical. At either crystal site of the two-crystal diffractometer space is available to accommodate medium size thermostats enclosing rigid goniometer heads. Because of the versatile design quite a variety of different X-ray experiments can be performed with the new diffractometer. Some examples will be given in paragraph 4 below.

2. Mechanical design

The instrument features the following design characteristics (fig. 1):

(1) The heart of the instrument is a rigid diffractometer bench T made of cast iron NiCr 202 alloy ensuring long term shape stability. Incorporated in the bench T are two parallel axes T1 and T2 each with coarse, fine, and superfine angular adjustment of crystals C1 and C2 for any kind of low, medium or high resolution two-crystal work. C1 and C2 are mounted on large goniometer heads T3 and T4, respectively. Both T3 and T4 feature ρ - and x -axes oriented at right angles to each other and with respect to the axes of T1 and T2 as shown in fig. 2. Furthermore, T3 and T4 permit x -, y -displacements in the plane perpendicular to the axes of T1 and T2. The bench T is strong enough and the separation of T1 and T2 is large enough to accommodate fairly heavy and spacious cryo- or thermostats around C1 and/or C2. The heads T3 and T4 are composed of separable modules if the sample size or some other necessity e.g. the use of an Eulerian cradle or similar would require to take off parts or all of the head.

(2) The direct beam R_i from the synchrotron source can be made incident on the monochromator M preceding crystal C1. M is mounted on the goniometer head M1 which is of the same design as T3 and T4. The Bragg angle Θ_M at the monochromator is adjusted by the drive ρ of M1 or by M2, depending on the orientation of the swing M3. Normally M is a multiply diffracting groove crystal with an even number of reflections or some other system of crystal reflections ensuring that the beam R_M diffracted by M remains parallel to R_i . Again, parts or all of M1 can be taken off in modular fashion if a monochromator of special design shall be employed.

(3) For adjustment with respect to the incident beam R_i (or R_M) the two-axes bench T is revolving about the axis of T1 by means of the drive T5. Back reflection geometry close to $\Theta = 90^\circ$ for high resolution $\Delta d/d$ or $\Delta E/E$ work (d : lattice parameter, E : energy) is possible.

(4) In order to permit the orientation of the diffraction plane of the two-crystal diffraction to vary between horizontal and vertical

it is possible to rotate the bench T about the incident beam R_i (or R_M) by means of the swing support T6.

(5) In a similar way the orientation of the diffraction plane of the monochromator can be chosen between horizontal and vertical by means of the semi-swing M3. Note that diffraction plane orientations can be adjusted independently for M and T, e.g. vertical for M and horizontal for T. An example where such an arrangement can be useful is the reduction of the scatter of the exciting radiation via its polarization state in fluorescence spectroscopy as described in paragraph 4.5 below.

(6) The solid state detector D is revolving about axis T1 (T2) by means of the drive D8 (D9), respectively. Drive D4 serves to rotate D about the axis of its dewar D2. With the leveling drive D5 the detector tube D1 is aligned to the height of the beam R_2 . Note that the distance between D8 and D9 equals that of T1 and T2 so that D can follow movements of T in a completely analogical way. On the other hand, by suitably combined adjustments of D8 and D9 the detector can trace any given path in the detector plane (the plane normal to the axes of D8 and D9).

(7) The swing D10 serves to rotate D about R_i in order to give the detector plane any orientation between horizontal and vertical. The function of D10 is thus similar to those of M3 and T6. Again the alignment of the detector plane is independent of that of the diffraction plane orientations of M and T. Hence, if required, D can easily measure also beams which are inclined to the diffraction plane of T or M. Another reason for providing a separate swing D10 is that the two-crystal bench T is better protected against mechanical noise caused by D or while moving D. In order to keep the detector dewar D2 from tilting too much when D is operated in a plane inclined by more than about 30° against horizontal, the detector tube D1 i.e. crystal and preamplifier, can revolve with respect to the dewar D2 by means of the inclination drive D3 as shown in fig. 3. Before operating D in the vertical plane, D has to be detached from D4, rotated by hand 90° about beam R_2 and then bolted again to D4.

(8) The base B of the instrument is a rigid welded iron structure providing support for the swing drives M3, T6 and D10 of monochromator, two-axis diffractometer bench, and solid state detector, respectively. The swing drives are ring-shaped so that in their centre a circular cross section 300 mm in diameter is free for the passage of beams including eventual beam pipes etc. On T and the swings there are ample thread holes provided for easy attachment of slits, additional beam pipes, absorber wheels and similar auxiliary accessories.

The monochromator M with its swing drive M3 can be located at four different positions P_1 to P_4 as shown in fig. 4. P_1 is the commonly employed position. Position P_2 is of interest if M and C1 have to be closer to each other and at the same time the back reflection range is not needed. P_4 is useful in high resolution inelastic X-ray scattering as explained in paragraph 4.3 below.

Drives B1 serve to adjust the common axis of the swings M3, T6, and D10 to the height and direction of the incoming beam R_i and to compensate an eventual parallel shift between R_i and R_M caused by the monochromator when it is diffracting in the vertical plane. In a similar way drives B2 are used for alignment of the instrument in the horizontal plane, which, in general, is less critical since R_i is usually extended horizontally but of limited height due to the relativistically compressed radiation cone of electrons emitting synchrotron radiation.

(9) Except for B2 all drives are equipped with stepping motors and encoded with either optical or inductive absolute digital encoders. The fine and superfine drives of T1 and T2 have analog absolute encoders. Operation is fully automatized by an on-line PDP 11/23 computer (see paragraph 3 below). The most critical movements have hardware safeguarded ranges with limiting switches operating directly on the stepping motor supply units. Increments per motor step and per encoder unit, ranges and approximate

maximum speeds are given for all drives in table 1. In order to maintain large accessible angular ranges of the swings special guiding devices feeding the numerous cables to all drives, encoders, and limiting switches located on swings had to be provided.

Fig. 5 is a photograph of the diffractometer complementing the information of the highly simplifying schematic illustrations of figs. 1 to 3. In building the instrument it was intended to incorporate commercially available mechanical subunits like diffractometer axes, translation stages, cradles etc. wherever possible. In the end, however, much less use of such units could be made than was hoped for initially. Main reasons for this were insufficient or unknown (undefined) strength of commercial components when operated in a plane other than horizontal, bulkiness at the strength required and/or lack of suitable encoding. In favourable cases as with the goniometer heads M1, T3 and T4 commercial translation stages^{†)} and cradles^{††)} could be incorporated after suitable modification and complementation.

Table 1. Drive Characteristics

drive	range [°]*	increment per motor step [arc sec]*	encoder unit [arc sec]*	approx max speed [°/sec]*
monochromator - θ M2	360	18	36	0.4
monochromator - swing M3	±180	18	3	4
two-axis bench				
T1, T2 { -coarse	±180	18	3	0.4
{ -fine	± 2.9	1	* *	0.3
{ -superfine	± 0.029	0.01	* *	0.003
T5	±180	2	6	0.4
detector				
D8, D9	±180	3.6	108	0.8
D3	±110	72	14.4	16
D4	360	54	108	12
swing drives				
T6, D10	±180	18	86.4	0.3
goniometer heads				
M1, T3, T4				
φ	± 30	12	6	0.2
α	± 30	36	6	6
x, y	± 27mm	125 μm	1 μm	13 mm/sec
leveling drives				
B1	400mm	0.21 μm	15 μm	75 mm/min
D5	± 40mm	0.84 μm	* * *	40 mm/min

* except stated otherwise, * * analog encoder 0.1 arc sec/mV, * * * no encoder

^{†)} furnished by Fa. Schneeberger & Co, Höfen/Enz
^{††)} furnished by Fa. Spindler & Hoyer, Göttingen.

3. Computer Control

The control system design follows some general specifications set by HASYLAB: For the entire laboratory a central computer (PDP 11/34) equipped with all necessary input/output hardware is provided. It will be linked to the instrument computers located at their respective stations in the experimental hall. These computers (preferably PDP 11/23) are to be installed with a minimum of input/output devices and use the CAMAC [2] system for control of the instrument. They shall be able to perform preliminary data processing for immediate feedback into the running experiment. The "post mortem" data analysis will be done by the central computer or at the experimentalist's home institution.

A set of special requirements is posed to the control system by the concept of the two-axis diffractometer itself:

- a) Service to about 40 stepping motors of different type and power (see table 1) of which some must move synchronously (e.g. two for each of the swings T6 and D10, up to four for lifting the base frame B1) and adequate service to the corresponding encoders.
- b) Radiation safety requires a lead hutch and an interlock system. Thus the geometrical configuration of all movable parts ought to be presented in an overview system with immediate-access manual control.
- c) Several X-ray detecting, counting or monitoring chains may be active simultaneously. All single digital and/or analogue data including those taken about sample temperature, DC-field (e.g. on ferroelectric crystals), shutter and window positions must constantly be at the computer's disposal.
- d) Ample memory space for the diffractometer control program system and for intermediate storage of direct and pre-processed data is needed.

- e) Bus systems should be used whenever feasible to reduce mechanical problems caused by bulky strings of connecting cables (see 2.9 above).

The above demands led to the concept shown in fig. 6:

- (1) A PDP 11/23 with 124 kBytes random access memory and two disc drives serves as a master computer supported by an 8086 microcomputer [3].
- (2) Identical CAMAC stepping motor controls with digital remote control input (BORER type 1162) are used, allowing easy replacement or exchange. Individual electric demands of the stepping motors are matched to the CAMAC modules by different power drives.
- (3) The radiation safety interlock with its lead hutch prevents supervising of motions by the experimentalist. To obtain knowledge of the actual geometrical configuration of the instrument it was decided to associate an encoder to each relevant motor drive. A "DISMOS" panel displays these encoder data with a high updating rate. Each single display unit consists of a LED display (up to 16 digits) with switch selectable format (e.g. degrees, divided into minutes/seconds or into decimals etc.). Push-buttons are provided for single step and continuous drive of the corresponding stepping motor in either direction. The "DISMOS" panel is managed independently by the 8086 microcomputer, thus permitting manual operation for testing and adjusting experimental set-ups which are not intended to perform under full computer control.
- (4) The intrinsic Ge single-crystal detector D (see 2.6 above) is supported by a multichannel analyzer Canberra 8100. Two additional scintillation detectors with single-channel discriminators can be employed at the same time. Both the MCA and the scintillation counters are linked to the computer to assure immediate availability of the counting data.

(5) Encoder data multiplexing units installed on each swing and two other places are also managed by the 8086 micro-computer. They drastically reduce the number of cables between the diffractometer and the electronic control equipment.

A technically oriented description of parts of the hardware as well as of the software system will be published separately [4,5].

4. Exemplary experiments

In this paragraph we describe the operation of the new diffractometer in a few typical experiments performed with synchrotron X-rays. The list is by no means exhaustive nor do we claim that we have reached in the set-ups sketched here the ultimate of optimization. Our main intention in presenting and describing exemplary experiments is to illustrate the instruments's versatility, and perhaps to stimulate some of the readers, to use it.

4.1 Two-crystal topography

This method of X-ray topography [6] has so far almost [25 - 27] exclusively been performed using the monochromatic radiation of characteristic X-ray lines.

When performed in the reflection (Bragg-case) geometry, two-crystal topography is particularly suited to detect and measure very small lattice deformations present within a thin surface layer of a crystal. A recent example is the quantitative determination of minute lattice strain of the order of $\Delta d/d = 10^{-8}$ (d : lattice parameter) frequently encountered in so-called perfect silicon crystals [7]. What can be gained by performing this technique with synchrotron radiation? In answering the question the following points can be made:

(1) The possibility of λ -tuning allows to vary the strain sensitivity and the penetration depth in a systematic way, which can help considerably in deducing the actual deformation state of the crystal from the intensity pattern on the topograph.

(2) By tuning λ on the absorption edges of atoms present in the crystal's matrix an eventual inhomogeneous distribution can be detected.

(3) Employing polarized radiation one can vary the penetration depth and the strain sensitivity at a given fixed wavelength.

(4) Because of the highly collimated radiation the image resolution can be increased for the same distance between photographic plate and specimen.

(5) Exposure times are expected to decrease by two to three orders of magnitude.

The set-up of the diffractometer for two-crystal topography is shown in fig. 7. Sample and reference crystal are mounted on T. A monochromator M is positioned at P_1 (fig. 4). For a given sample material the wavelength band contributing to the topograph is determined by the choice of material and reflection for M. Since R_1 is usually highly polarized in the horizontal plane, in order to optimize the intensity, M, C1 and C2 should diffract in the vertical plane as drawn in fig. 7. At the sacrifice of intensity the strain sensitivity of the method may be increased by letting C1, C2 diffract in the horizontal plane and their Bragg angle approach 45° , which by tuning the wavelength through rotation of M about M2 is always possible.

4.2 Inelastic X-ray scattering: medium resolution [8]

The experimental arrangement shown in fig. 8 can be used in order to measure Compton-, plasmon- and resonant Raman-scattering of X-rays.

Mounted on axis M2 at location P_1 (fig. 4) is the monolithic monochromator M with two asymmetric reflections as shown in fig. 8. M monochromatizes the incident beam and at the same time reduces the beam height by a factor of ten to about 1 mm, thereby making the sample S on axis T1 of the diffractometer a source of scattered radiation with effective slit geometry. In order to facilitate the second asymmetric reflection of M the

perfect crystal intrinsic curve for that reflection must be widened by suitable surface treatment like grinding or similar.

The inelastically scattered radiation is analyzed by the curved crystal analyzer A mounted on axis T2 of the diffractometer together with the detector D on its proper axis D4 (fig. 1). Sample, curved analyzer crystal, and the slit in front of D fulfil the well-known Rowland circle geometry often used in ordinary X-ray spectrometry as indicated in fig. 9. For any given scattering direction at S, the spectrum of scattered radiation is scanned by making A and D perform suitably correlated translations and rotations so that the Rowland geometry is maintained throughout the scan. Since all movements of T and D are encoded and computer controlled it is not difficult to accomplish correlated movements as required.

With Compton scattering, in measuring the doubly differential cross section $d^2\sigma/d\omega d\Omega$ (ω : energy, Ω : solid angle), typical values are: incident energy $\omega_1 > 20$ keV, energy transfer $\omega \approx 2$ keV, momentum transfer $q \approx 10$ at units, useful momentum resolution $\frac{\Delta P}{P_F} = 0.05$ to 0.1 (P_F : Fermi-momentum). With these values an energy resolution $\frac{\Delta E}{E} \approx 5 \times 10^{-4}$ is required. Assuming 0.35 mrad vertical divergence of the beam R_1 incident from the storage ring and employing Germanium crystals at M and A the above value of $\frac{\Delta E}{E}$ is achieved with Bragg angles $\theta_{BM} = 35^\circ$ at M and $\theta_{BA} = 76^\circ$ at A which is quite feasible with the new diffractometer.

In the case of plasmon- and Raman-scattering, typically $\omega_1 \approx 5$ keV, $\omega \approx 5$ to 50 eV, $q \approx 0.2$ to 1.5 at units and $\frac{\Delta q}{q_c} = 0.05$ to 0.1 (q_c : Plasmon cut-off vector, ≈ 0.5 at units), with a desired $\frac{\Delta E}{E} \approx 10^{-4}$, what could be achieved by making $\theta_{BA} \approx 74^\circ$ and $\theta_{BM} \approx 87^\circ$.

4.3 Inelastic X-ray scattering: high resolution [8,9,10]

Resolutions $\Delta\omega \approx 100$ meV to 5 meV in energy transfer appear to become accessible if extreme backscattering geometries are used. Such measurements could be of value in studies of lattice vibrations and low energy solid state or molecular excitations, a realm so far chiefly investigated by thermal neutron scattering.

Differentiating Bragg's equation one obtains $\Delta E/E = -\Delta\theta_B \cot \epsilon_B$ a result, which, when naively interpreted suggests that extremely large energy resolutions with even relatively large $\Delta\theta$ (divergent beams) could be obtained at or near $\theta_B = 90^\circ$. However, a proper treatment of the backreflection with the dynamical theory of X-ray diffraction [9] yields that (for a plane wave) $\Delta E/E = |\chi_h|$ independent of $\epsilon = 90^\circ - \epsilon_B$, the deviation from exact $\epsilon_B = 90^\circ$, where χ_h is the Fourier coefficient of the electric susceptibility χ .

Furthermore, for ϵ smaller than a few mrad the range $\Delta\theta$ of total reflection is no longer proportional to $|\chi_h|$ (as at large ϵ) but rather to $|\chi_h|^{1/2}$ which, with typically $|\chi_h| \approx 2.5 \times 10^{-7}$ (Si 888, $\epsilon_B = 90^\circ$) gives an about 2000 times larger reflectivity than one would obtain from $\Delta\theta$ proportional to $|\chi_h|$. Hence, in spite of the generally low intensity of high order reflections, yet reasonable intensity can be expected in the extreme back reflection range [9]. At the same time, in the above example, $\Delta E/E \approx 2.5 \times 10^{-7}$ and, with $E = 15.8$ keV, $\Delta E \approx 4$ meV, which is extremely small. Hence it is to be expected that in the near future X-ray inelastic scattering will be extended down to energy transfers of the order of 10 meV. Needless to say that, in order to accomplish this, synchrotron X-rays must be used since with characteristic radiation λ -tuning is impossible and above all the intensities would be too low.

The realization of backreflection geometry with the two-axis diffractometer is illustrated in fig. 10. The sample is mounted on axis T1. The main difficulty in backreflection is to let the incident and the analyzed beam pass the specimen. By locating M at P₄ (fig. 4) and using a simple rigid extension arm bolted to T2 for mounting the analyzer A, deviations from 90° of the Bragg

angles at the monochromator, ϵ_M , and at the analyzer, ϵ_A , respectively, of no more than about 2 to 4 mrad appear feasible. Energy resolutions of the order of 5 to 10 meV should then be achievable at reasonable intensities, e.g. with DORIS operating at 3.5 GeV, 50 mA [9].

4.4 Inelastic X-ray scattering at Bragg-position

With the set-up shown in fig. 11 the Compton scattering of a perfect crystal could be measured near the Bragg-position [11]. From the data obtained information about the nondiagonal elements of the first order momentum space density matrix can be derived [12]. The sample is mounted on axis T1 and the dynamic reflection range is monitored by the detector D. Compton scattered radiation is analyzed by the bent crystal analyzer combined with a position sensitive detector mounted on axis T2. The incident radiation is monochromatized by the usual grooved monochromator M on axis M2 at position P1.

4.5 Fluorescence spectroscopy with polarization suppressed exciting radiation

Fig. 12 illustrates the set-up of the diffractometer in this case. The monochromator M at position P1 is diffracting in the vertical plane. The sample is located at T1. The fluorescence radiation is observed in the horizontal plane at 90° against R₁ by means of the analyzer on T2 combined with the detector D. Since the exciting radiation is linearly polarized parallel the line connecting T1 and T2 it is highly suppressed for the analyzing spectrometer.

4.6 High resolution small angle scattering with point geometry

Fig. 13 illustrates the small angle scattering camera with crystal collimation of beams [13]. Because of the high intensity of synchrotron radiation the camera may be used in so-called point-

geometry, i.e. with a third grooved crystal G3 interposed between the main multiply reflecting grooved crystals G1 and G2 located on axes M2 and T2. While G1 and G2 diffract in the vertical plane, G3 is diffracting in the horizontal plane. G3 is, with the sample between the walls of the groove, located on axis T1.

With a solid state detector scattering curves obtained with a set of harmonics can be measured simultaneously, which gives additional information about the sample.

4.7 Two-crystal high resolution diffractometry [14,15]

With two identical crystals C 1 and C 2 and a diffraction geometry as in fig. 14 employing Bragg scattering at the two antisymmetric vectors \underline{h} and $-\underline{h}$, the dispersion-free double-crystal case [16] can be used. This set-up allows to measure small variations of lattice constants $\Delta^d/d = -\cot \theta \cdot \Delta\theta$ with a resolution of the order of 10^{-8} . It is mainly limited by the temperature constancy of C 1 and C 2 (10^{-3} K) and by their quality permitting to measure a small $\Delta\theta$ at high Bragg angles θ (typically 85 to 88°), aimed at by tuning λ .

4.8 Medium resolution powder diffractometry [17, 18]

One axis (T1) supports a powder sample. Between T 1 and the detector, a Soller slit system is mounted. It reduces systematic reflection profile distortions due to divergence of scattered radiation perpendicular to the plane M-C1-D [19]. This ensures a resolution of about 0.002° in back-reflection geometry which for each reflection of the sample is obtained by λ -tuning. With a Δ^d/d of about 10^{-5} , lattice deformations caused by strain (e.g. in metal sheets) can be investigated [17].

4.9 Dispersion-free single-crystal Bragg intensity measurements [16]

Standard integrated diffraction intensity measurements used for crystal structure determination can easily be performed on the two-axis diffractometer equipped with a suitable monochromator crystal. None of the special features of the instrument is employed for this purpose. If, however, similar to fig. 7 two identical crystals C 1 and C 2 are used and set

to scattering vectors \underline{h} and $-\underline{h}$ (or \underline{h}_1 and $-\underline{h}_2$ with $|\underline{h}_1| = |\underline{h}_2|$), then a dispersion-free (or nearly dispersion-free) intensity measurement can be achieved by scanning the Bragg reflection profile of C 2. This permits collecting very small Bragg intensities above a relatively low background [20]. This technique is, for example, helpful in measuring the so-called "forbidden reflections" (e.g. (222) in diamond) which are extinguished for spherical (and spherically vibrating) atoms in some special equipoints. Another application is to measure low elastic scattering from incommensurate phases. In both cases, the high primary beam R_M intensity is used.

4.10 Single-crystal diffractometry with alternating wavelengths: "Lambda method" [21,22]

This technique employs Bragg intensity differences between two or three wavelengths appropriately selected around the absorption edge of one species of atoms (called "edge atoms") in an unknown crystal structure. It yields directly two types of interatomic vectors separated in two Fourier transforms of the $\Delta|F(\underline{h})|^2$ data sets: those between the edge atoms leading to their positions in the unit cell [23] and others between each edge atom and each "normal" atom providing pictures of the normal atom arrangement as seen from each edge atom. This comprises a partial (or in favourable cases: complete) circumvention of the "phase problem" in crystal structure analysis.

A simple arrangement for this type of measurements contains a fore monochromator capable of fast switching between two or three wavelengths (with $\Delta\lambda/\lambda$ resolution of approximately 10^{-3}) maintaining height and direction of R_m (fig. 1). R_m is monitored by a second detector. An Eulerian cradle or

similar device on T 1 permits measuring Bragg intensities of all reflections in the asymmetric part of reciprocal space (including Bijvoet-equivalents).

Applications for this "lambda method" range from straightforward crystal structure determinations in otherwise difficult cases (automatically including correct absolute configuration and/or polarity of enantiomorphous or polar molecules) via partly ordered atomic arrangements (e.g. fast ionic conductors) to amorphous materials (selected atomic pair distribution functions [24] in binary alloys).

5. Acknowledgement

We wish to thank U. Dretzler (Dortmund) and G. Ernst (Dortmund) who designed and constructed most of the mechanics, and Dr. S. Heinrich (Saarbrücken) who designed and built most of the electronic system, for their enthusiastic cooperation. Two grants (BO 05463 and Fi 05109) from the Minister of Research and Technology (BMFT) of the Federal Republic of Germany permitted to bring our ideas to reality. Helpful discussions with colleagues and coworkers at our home institutions and at HASYLAB and their assistance in practical details are acknowledged.

References

- 1 U. Bonse and K. Fischer, Proposal to the Federal Minister of Research and Technology, January 1978 in "European Synchrotron Radiation Facility, Supplement III Instrumentation", B. Buras and G.V. Marr Eds., European Science Foundation Strassburg 1979, page 98.
- 2 J.G. Oules, *Elektronik* 19 (1970) 335 and 387; 20 (1971), 53; 23 (1974) 327.
- 3 Intel Corporation (1978) 9800698 A
MCS-86 system design kit user's guide; 9800722 B
MCS-86 system user's manual.
- 4 S. Heinrich, in preparation
- 5 S. Heinrich and W. Schildkamp, in preparation
- 6 U. Bonse and E. Kappler, *Z. Naturforschg.* 13a (1958) 348
U. Bonse, *Z. Physik*, 153 (1958) 278
- 7 U. Bonse and I. Hartmann, *Z. Kristallogr.* 156 (1981) 265.
- 8 W. Schülke, to be published
proposal to the HASYLAB synchrotron radiation reviewing board, Oct. 1980
- 9 W. Graeff and G. Materlik, *Proc. Nat. Conf. on Synchrotron Radiation Instrumentation*, Ithaca, N.Y. July 1981;
to be published in *Nucl. Instr. Meth.*
- 10 D. Moncton, *Summer School on X-Ray Scattering with Synchrotron Radiation*, Vienna, Sept. 1980, ESF sponsored
- 11 W. Schülke and U. Bonse
Acta Cryst. A37 (1981) C132
- 12 W. Schülke, *Physics Letters* 83A (1981) 451
- 13 U. Bonse and M. Hart in *Small Angle Scattering*,
H. Brumberger ed., Gordon & Beach (1966) 121

- 14 H. Wern, Master's Thesis, University of Saarbrücken, 1980
- 15 K.H. Ehses, H. Wern and W. Schildkamp, 1980
Annual Conf. of the Condensed Matter Division (EPS), Antwerp;
in press (Plenum Publishing Corp., New York)
- 16 W. Schildkamp, K.H. Ehses and H. Wern, Z. Kristallogr. 156 (1981) 99
- 17 H. Ruppertsberg, W. Schmidt and H. Weiland, Z. Metallkde. 71 (1980) 475
- 18 H. Ruppertsberg, in "Proceedings of the Second European Conference on
Non-Destructive-Testing"., Vienna 1981, to be published
- 19 H. Klug and L. Alexander, X-Ray Diffraction Procedures,
J. Wiley & Sons, New York (1974)
- 20 H. Wern, private communication, 1980
- 21 K. Fischer, A. Ribbens, J. Spilker, G. Schäfer,
Z. Kristallogr. 156 (1981) 3
- 22 K. Fischer, Acta Cryst. A37 (1981) C308
- 23 T. Sakamaki, S. Hosoya and T. Fukamachi, Acta Cryst. A36 (1980) 183
- 24 P. Chieux, H. Ruppertsberg, J. de Physique 41, C8 (1980) 145
- 25 W. Parrish and C. Erickson, Acta Cryst. A34 (1978) S331
- 26 J. Miltat and M. Kléman, J. Appl. Phys. 50 (1979) 7695
- 27 J.F. Petroff, M. Sauvage, P. Riglet and H. Hashizume, Phil. Mag. A42
(1980) 319

Figure captions

- Fig. 1 Multi-purpose two-axis diffractometer for synchrotron X-rays at DORIS, schematic design. Top: side-view, bottom: view down on the instrument.
M: monochromator, M1: goniometer head of M, M2: θ -drive of M, M3: swing-drive of M.
T: two-axis double-crystal diffractometer bench, C1 and C2: first and second crystal of T respectively, T1 and T2: θ -drive of C1 and C2 respectively, T3 and T4: goniometer head of C1 and C2 respectively, T5: θ -drive of T, T6: swing drive of T.
D: solid state detector, D1: detector tube of D with crystal and preamplifier, D2: dewar of D, D3: inclination drive of D1, D4: θ -drive of D, D5: leveling drive of D, D6: detector bench, D7: detector arm, D8 and D9: θ -drive of D6 and D7 respectively, D10: swing drive of D.
B: base structure of the diffractometer, B1: leveling drives of B, B2: horizontal shift drives of B.
 R_i : beam incident from synchrotron source, R_M : beam diffracted by M, R_1 : beam diffracted by C1 and incident on C2, R_2 : beam diffracted by C2 and incident into D.

Fig. 2 Goniometer heads T3, T4 and M1, schematically. Definition of ρ - and x -axes and of x - and y -translations.

- Fig. 3 Function of inclination drive D3 for rotation of the detector tube D1 (crystal and preamplifier) against the dewar D2.
a): view in the direction of the X-ray beam,
b): view at right angles to the beam.

Fig. 4 Possible locations P_1 to P_4 of the monochromator M. Distances are drawn to scale. The shaded area is blocked by the swing drives and their supports.

Fig. 5 Photograph of the diffractometer. Detector D including detector arm D7 and goniometer heads T3, T4 (fig. 1) have been taken off. The monochromator is beyond the picture frame to the left.

Fig. 6 Two-axis diffractometer control system lay-out [4]

Fig. 7 Set-up of the diffractometer for double-crystal topography. The monochromator M is at position P_1 of fig. 4. Reference crystal C1 and sample crystal C2 are normally of the same, M is of the same or a different material. P: photographic plate, D: detector, compare with fig. 1 for the rest of notations. Drawn is the vertical plane.

Fig. 8 Set-up for inelastic X-ray scattering with medium energy resolution, axes T1, T2 are horizontal. Notations as in fig. 1.

Fig. 9 Maintaining Rowland circle geometry for inelastic X-ray scattering, see text. Notations as in fig. 1.

Fig. 10 Set-up for inelastic X-ray scattering with high energy resolution, back-reflection geometry. P1, P4 indicate the possible locations of the monochromator of fig. 4. Beam stop is at P1. Notations as in fig. 1.

Fig. 11 Set-up for inelastic X-ray scattering near Bragg-position, see text. Drawn is the vertical plane. Notations as in fig. 1.

Fig. 12 Set-up for fluorescent spectroscopy with polarization-suppressed scatter of the exciting radiation. Drawn is the horizontal plane. Notations as in fig. 1.

Fig. 13 Set-up for high resolution small angle scattering with point geometry. Drawn is the vertical plane. The groove crystal at T1 is diffracting in the horizontal plane. Notations as in fig. 1.

Fig. 14 Set-up for high resolution two-crystal diffractometry. Drawn is the horizontal plane. Notations as in fig. 1.

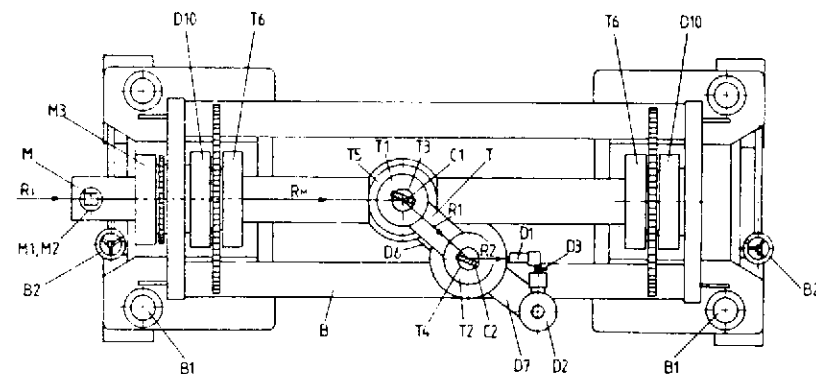
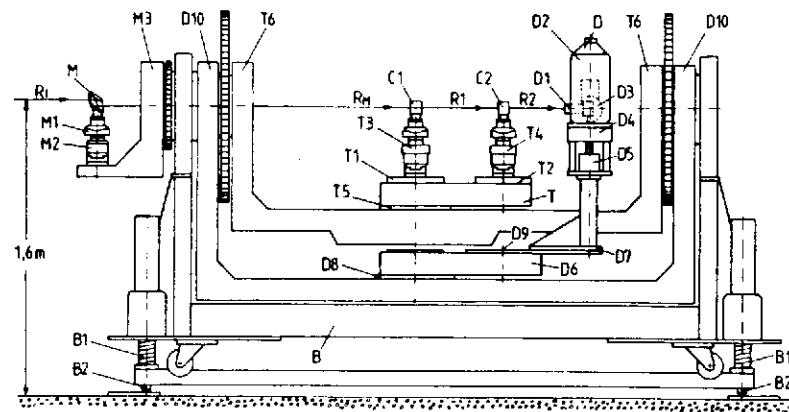


Fig. 1

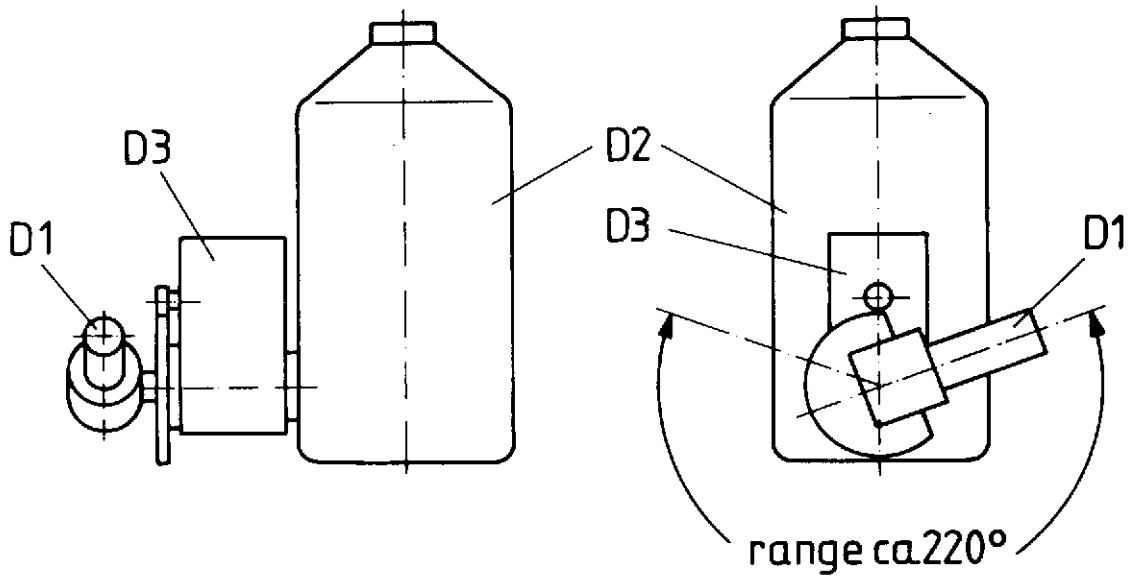


Fig. 3

a)

b)

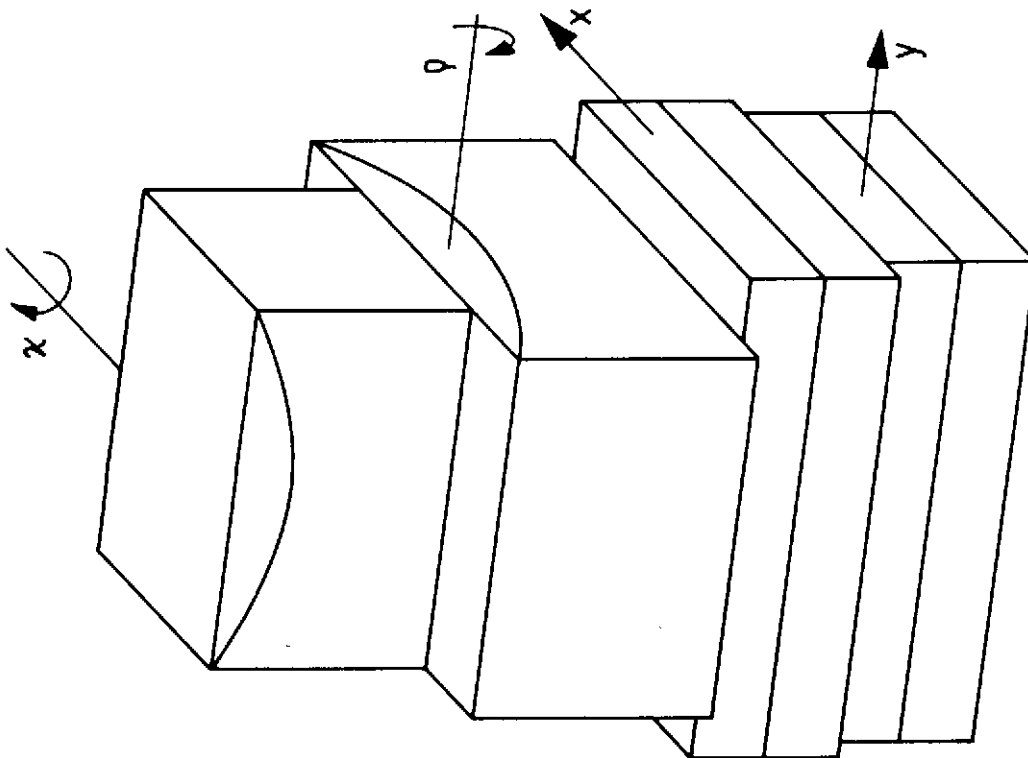


Fig. 2

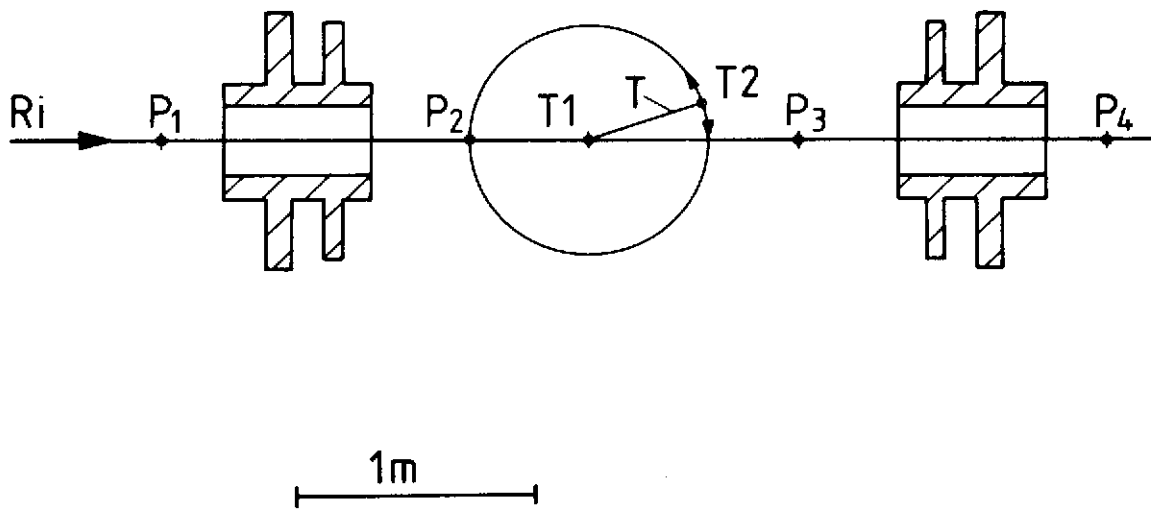


Fig. 4

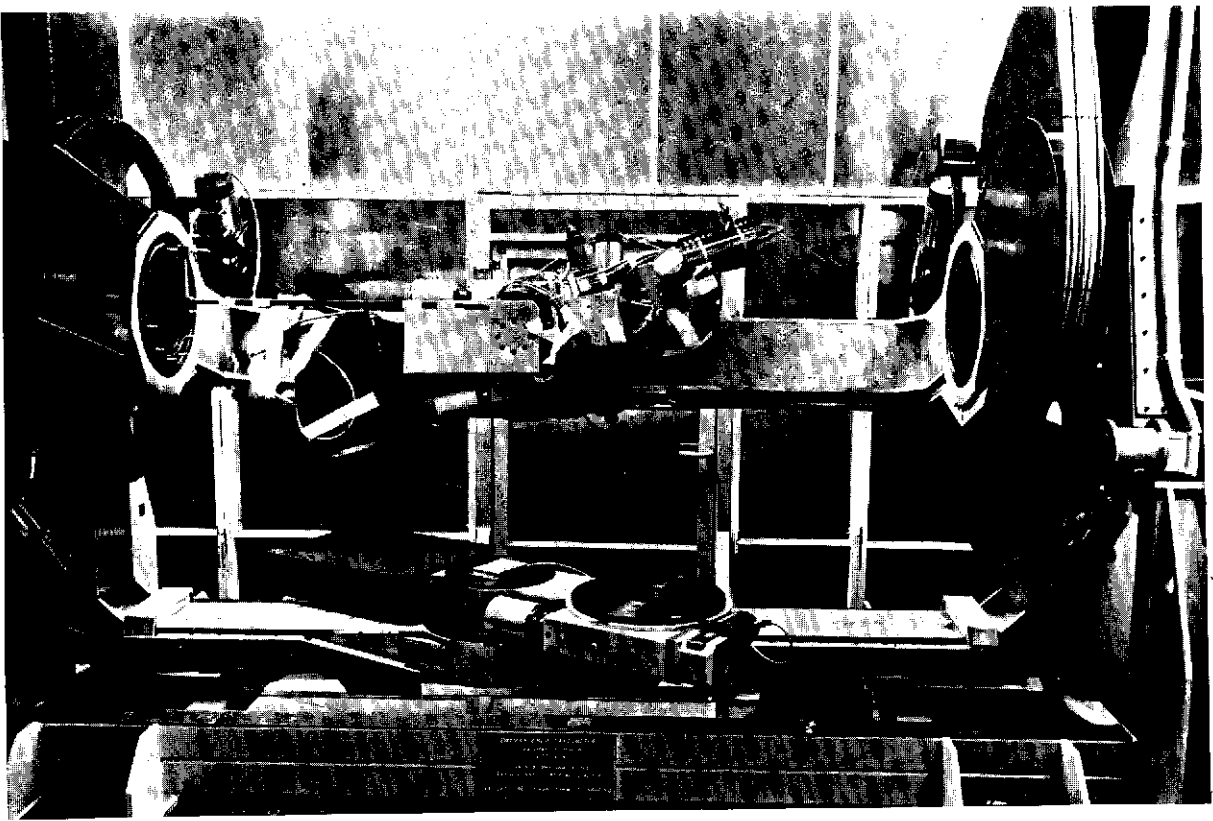


Fig. 5

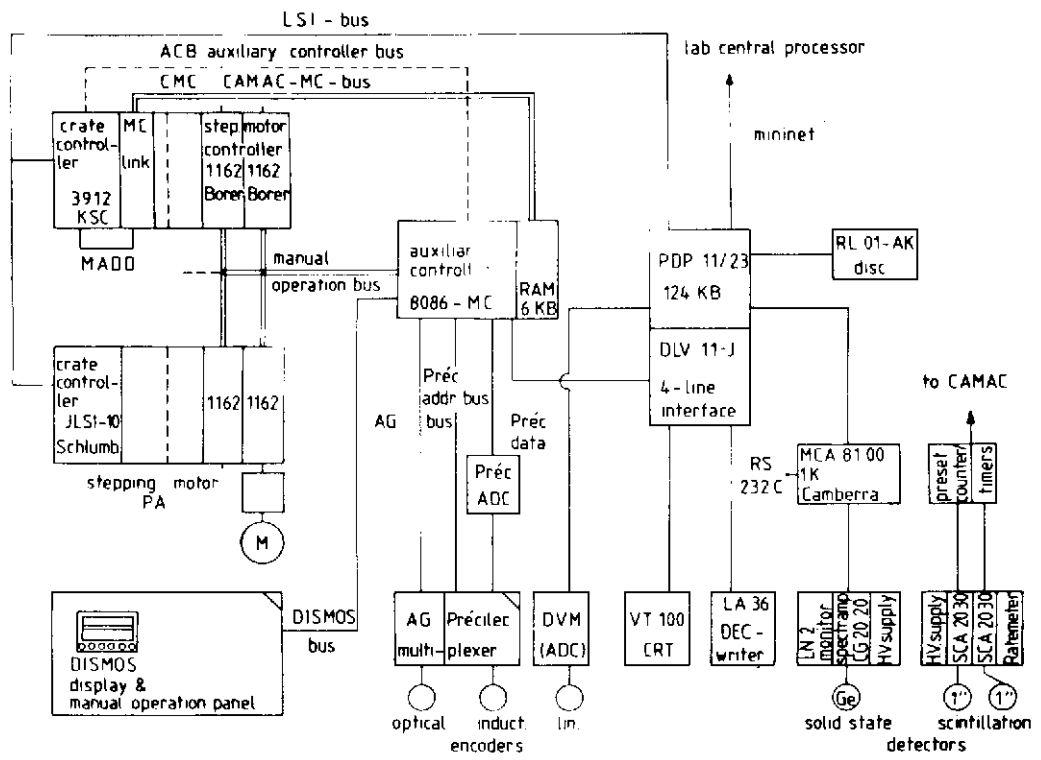


Fig. 6

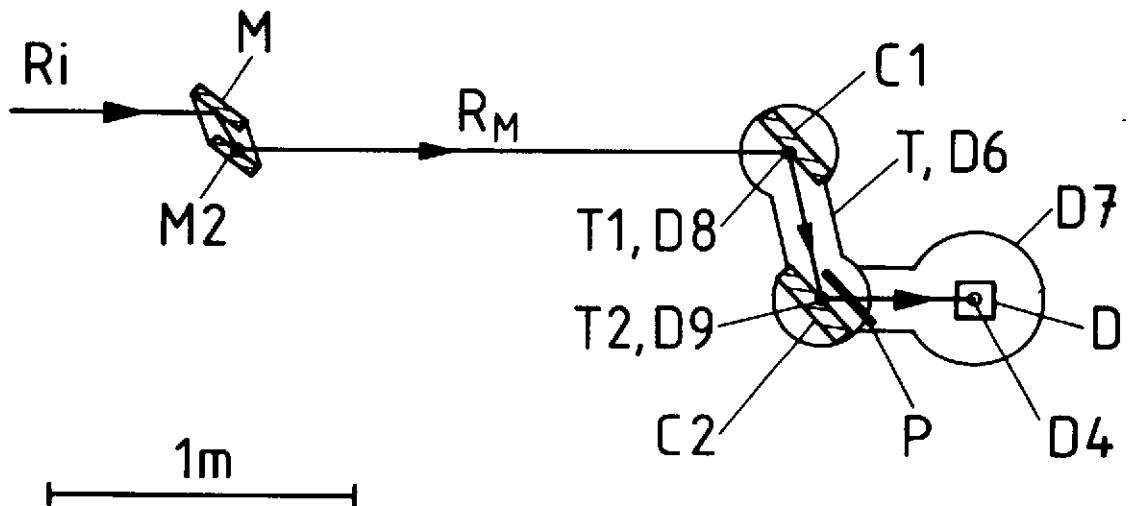


Fig. 7

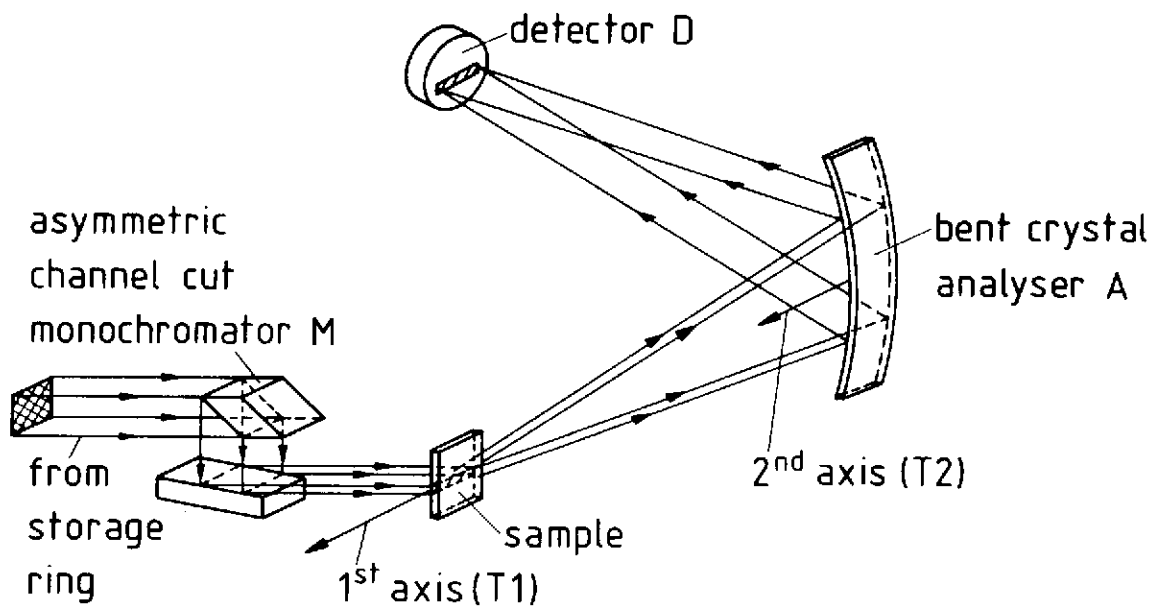


Fig. 8

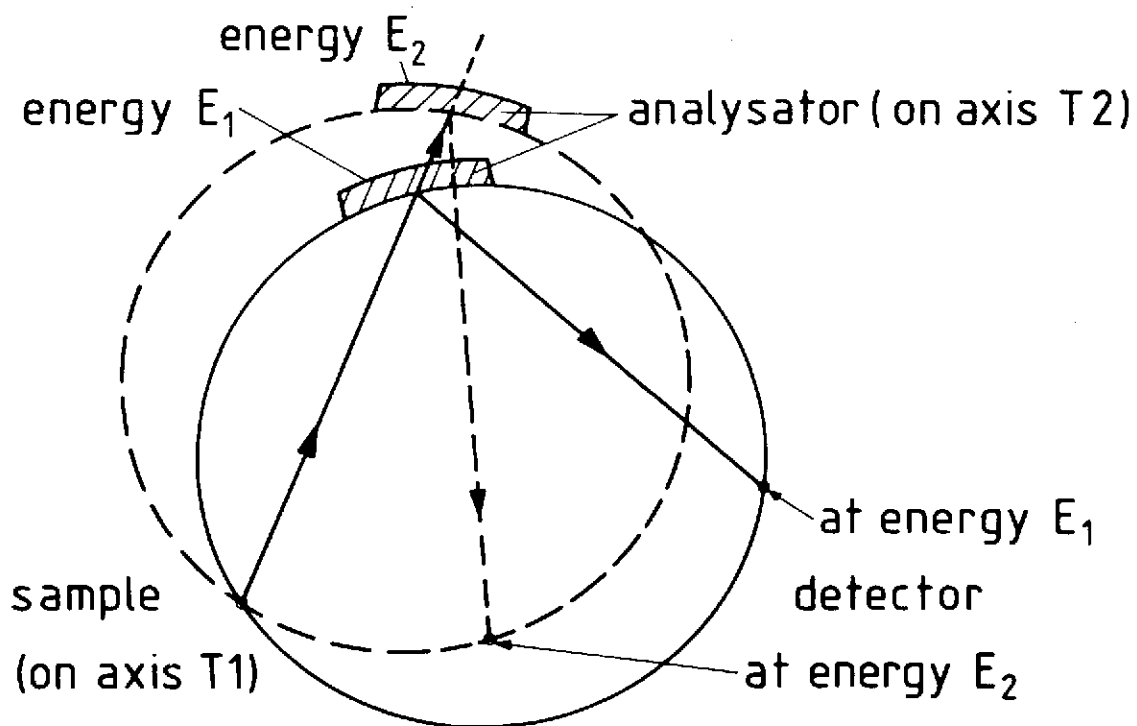


Fig. 9

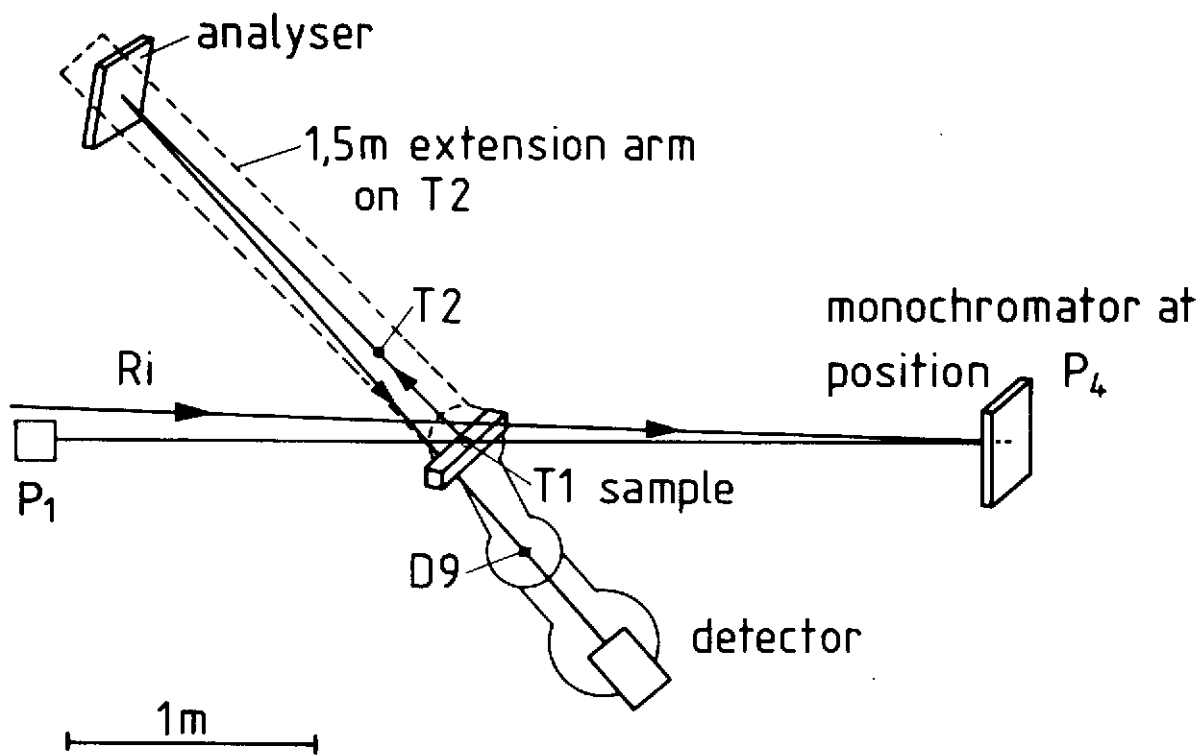


Fig. 10

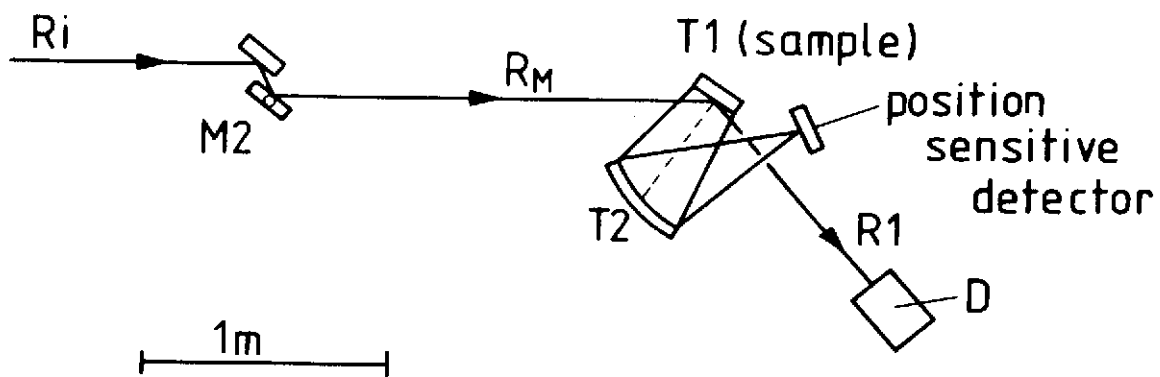


Fig. 11

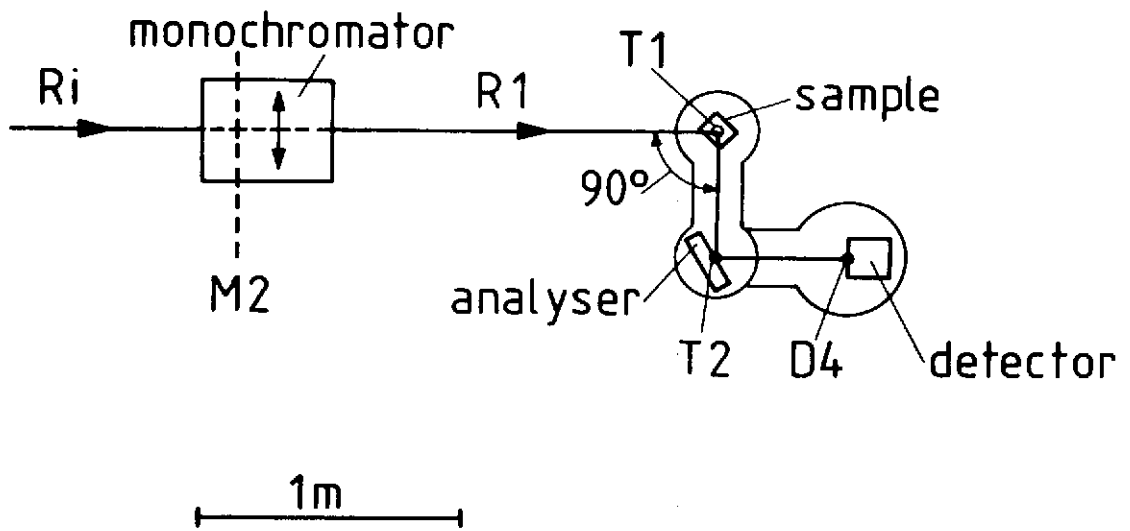


Fig. 12

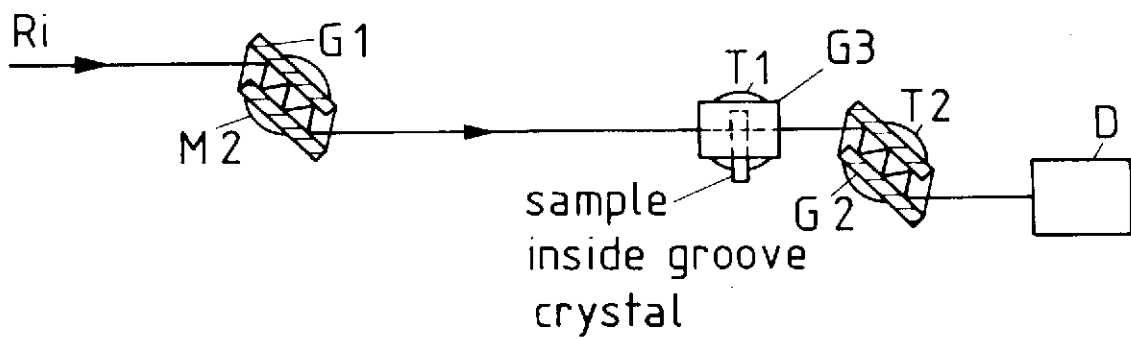


Fig. 13

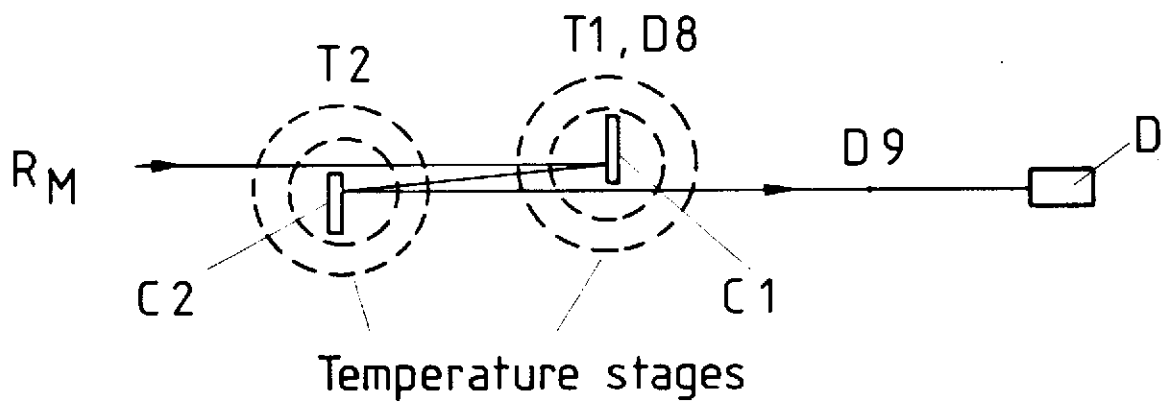


Fig. 14